Geochemical Journal, Vol. 29, pp. 301 to 315, 1995

The carbon-sulfide-iron relationship and sulfate reduction rate in the East China Sea continental shelf sediments

KUO-MING HUANG and SAULWOOD LIN

Institute of Oceanography, National Taiwan University, #1, Roosevelt Rd., Sect. 4, Taipei, Taiwan

(*Received October 6, 1994; Accepted May 26, 1995*)

Carbon/sulfide/iron relationship and sulfate reduction rate were investigated in the East China Sea continental shelf sediments. The area is characterized by median to high sulfate reduction rate, and high concentrations of iron oxide minerals. Organic carbon was found to be the primary limiting factor for the pyrite formation.

Sulfate reduction rate increased with increasing organic carbon concentration. C/S ratio displays a typical normal marine sediment ratio. Low DOP values and abundance of highly reactive iron oxide, ferrihydrite and lepidocrocite, indicate that iron is not limited in the East China Sea continental shelf.

INTRODUCTION

Sulfate reduction in continental shelf sediments plays an important role in the global sulfur and carbon cycle. The continental shelf receives more than 80% of the total organic carbon (157×10^{12} g/year) from the world's major rivers (Berner, 1982). A major portion of this organic carbon as well as that produced in the water column are consumed by anaerobic sulfate reduction in shelf sediments (Berner, 1982; Jorgensen, 1982). Consequently, most authigenic pyrite is deposited in continental shelf sediments (Berner, 1982; Lin and Morse, 1991). The deposition of pyrite and organic carbon in sediments underneath oxygenated sea water often produces a strong chemical signature, a constant C/S ratio. This ratio (C/S = 2.8) has been widely used in the interpretation of both modern and ancient deposition environment (Berner, 1970, 1982, 1984; Leventhal, 1983; Berner and Raiswell, 1984; Raiswell and Berner, 1985; Gautier, 1986; Dean and Arthur, 1989) as well as a fundamental base for modeling the atmospheric oxygen evolution over geologic time (Berner and Raiswell, 1983; Berner, 1989, 1991).

Despite the continental shelf being a primary sulfide depositional environment, no data is available on sulfate reduction rate and the factor(s) controlling pyrite formation in the East China Sea continental shelf sediments. The purpose of this study is to investigate sulfate reduction and to analyze the factors influencing pyrite formation in the East China Sea continental shelf sediments, in order to expand our present knowledge of pyrite formation in the continental shelf environment.

STUDY AREA AND ANALYTICAL METHODS

The East China Sea continental shelf is one of the largest shelf systems in the world. The principal sources of the fine-grained sediment in the East China Sea continental shelf are the Yantze River (5×10^8 tons/year) along with a very limited supply of not more than 0.06×10^8 tons/year from other small rivers (Li *et al.*, 1991). A large portion of this sediment supply is moved southward by the Jian-Su coastal current (Cao *et al.*, 1989). Part of the suspended sediments are transported east and northeast into the East China Sea area (Sternberg *et al.*, 1985). Fine-grained sediments are distributed off the Yantze River mouth and southward along the coast (Lee and Chough, 1989).

Shelf sediment samples (Fig. 1) were collected

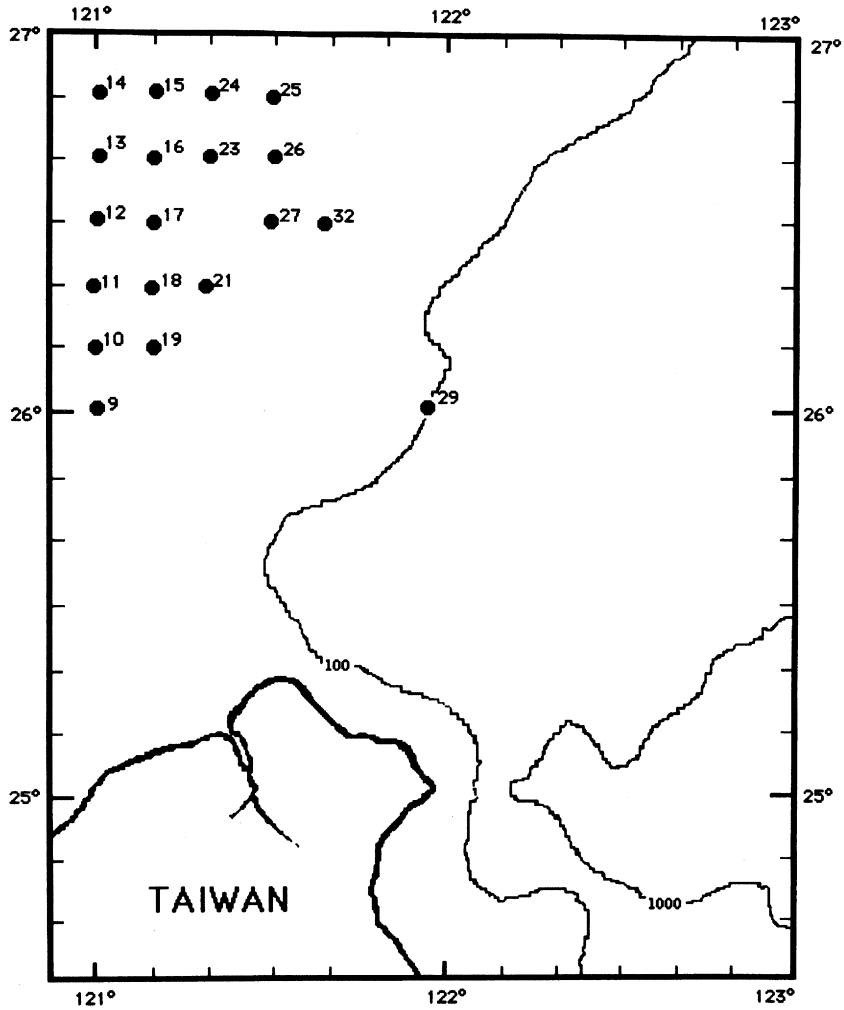

Fig. 1. Study area and sampling sites.

on board the R/V Ocean Researcher-I (16 stations, Cruise 322, July, 1992) using a box core or piston core. Subcored sediments were sectioned, usually 2 cm, in a nitrogen-filled glove bag (Aldrich) immediately after retrieving the box core on board. Subsectioned samples were injected with 1–2 μCi $Na_2{}^{35}SO_4$ (NEN, DuPont) and incubated for 24 hours at 22°C in the dark. After the incubation, samples were kept frozen in the refrigerator. Pore waters samples were centrifuged (4000 rpm, 15 minutes), filtered (Nuclepore, 0.45 μm) and stored in polyethylene (PE) vials at 4°C. All other sediments were stored frozen in PE centrifuge tubes for drying on land. After being freeze-dried for one week using a Labconco Freeze-drier, sediments were ground to powder using an agate mortar and stored in polypropylene vials for organic carbon, carbonate carbon and metal determinations.

Pore water sulfate was determined by ion chromatographic method (O'Dell *et al.*, 1984) using a Dionex 4500i Ion Chromatography equipped with a conductivity detector and IonPac AS4A anion exchange column. The effluents were 1.7 mM $NaHCO_3$ and 1.8 mM Na_2CO_3 with 0.025 N H_2SO_4 as regeneration fluid. All samples were

pre-diluted 100 times prior to analysis. The injection volume was 5 μl, and the precision of sulfate analysis is 0.4%.

Solid phase analyses included iron sulfide, iron, organic carbon and carbonate carbon determinations. Organic and carbonate carbon were analyzed using infrared determination of CO_2 evolved from high temperature (1400°C) combustion with a LECO SC-444 carbon/sulfur analyzer. Approximately 0.25 g of dry sediment was pre-acidified with ~2 ml of 6 N HCl to remove carbonate carbon. After drying on a hot-plate for 8 hours at ~60°C, the sample was combusted in a LECO carbon analyzer to measure its organic carbon content. Samples were analyzed directly without acid treatment to determine the total carbon concentration. Carbonate carbon was derived from the difference between total and organic carbon. The LECO carbon standard (502–062) was used for calibration. The average analytical precision was 0.88% (1 SD).

Pyrite-sulfur was determined using Cr(II) + 6 N HCl method (Cornwell and Morse, 1987; Canfield *et al.*, 1986). Approximately 5 g of wet sediment was distilled in an oxygen-free vessel for one hour. The H_2S evolved from boiling acid distillation was carried to the SAOB (sulfide antioxidant buffer, Orion) trap with high purity nitrogen (99.9%), and titrated with $Pb(ClO_4)_2$ (27.3 mM) using a Metrohm 686 titrator. The precision was better than 1.5% (n = 12) based on a sulfide standard (Na_2S, Sigma).

The rate of sulfate reduction was measured according to Lin and Morse (1991) and Jorgensen (1978). Extraction step was similar to the pyrite-sulfur distillation as described above. The evolved $H_2{}^{35}S$ was trapped in Zn-acetate (0.28 M). Activity of $Zn^{35}S$ and the remaining $^{35}SO_4$ were analyzed using a Liquid Scintillation Counter (Packard 1600TR).

Iron concentrations were determined using a scheme similar to Canfield (1989b). Oxalate iron was extracted with buffered 0.2 M ammonium oxalate + 0.1 M oxalic acid for 4 hours. Cold acid extractable iron was extracted with 1 N HCl for 16 hours (Lin and Morse, 1991). Total iron was digested using a CEM microwave digestion system (MDS-2000) with 2.5 ml of HNO_3:HF (5:2) and 10 ml of 4% H_3BO_3 mixture (Kokot *et al.*, 1992). After the extraction, iron was determined with a Atomic Absorption Spectrometer (Hitachi 8100Z). Total iron recovery from the NIST 1646 and BCSS-1 standard sediments were 95 ± 3% (n = 18).

Results

Sulfate reduction rates, pyrite-sulfur, organic carbon, pore water sulfate, reactive iron from stations 10, 13, 16, 17, 26 and 32 are shown in Figs. 2, 3 and 4. All data are also presented in Appendix.

Sulfate reduction rate and pyrite-sulfur

Rates of sulfate reduction and pyrite-sulfur concentrations versus depth are presented in Fig. 2. Sulfate reduction rate varied from 0.2 μM SO_4^{2-}/day to 40 μM SO_4^{2-}/day. Sulfate reduction rates in the study region were lower than those observed in the organic-rich coastal Cape Lookout Bight and the fine-grained, high sedimentation rate Mississippi Delta sediments but higher than most shelf sediments (see Canfield, 1989a; Reeburgh, 1983; Lin and Morse, 1991). A sub-surface sulfate reduction maximum was always observed at a depth of about 5–15 cm in each station. Double rate peaks were observed—one at or near the surface and a more frequently observed second maximum deeper down the core (Fig. 2). The surface maximum is approximately 30 to 90% of the subsurface peak rate.

Pyrite-sulfur was relatively low in the upper 10 cm and gradually increased with increasing depth. The increase in pyrite-sulfur always appeared at or underneath the sulfate reduction rate maximum, indicating an authigenic origin of pyrite. The concentration of pyrite-sulfur was in the range of 2–100 μmol/g, similar to those in the anoxic Gulf of Mexico sediments (Lin and Morse, 1991). No dissolved sulfide was found throughout the study area. This may result from the high concentration of reactive iron found in the region

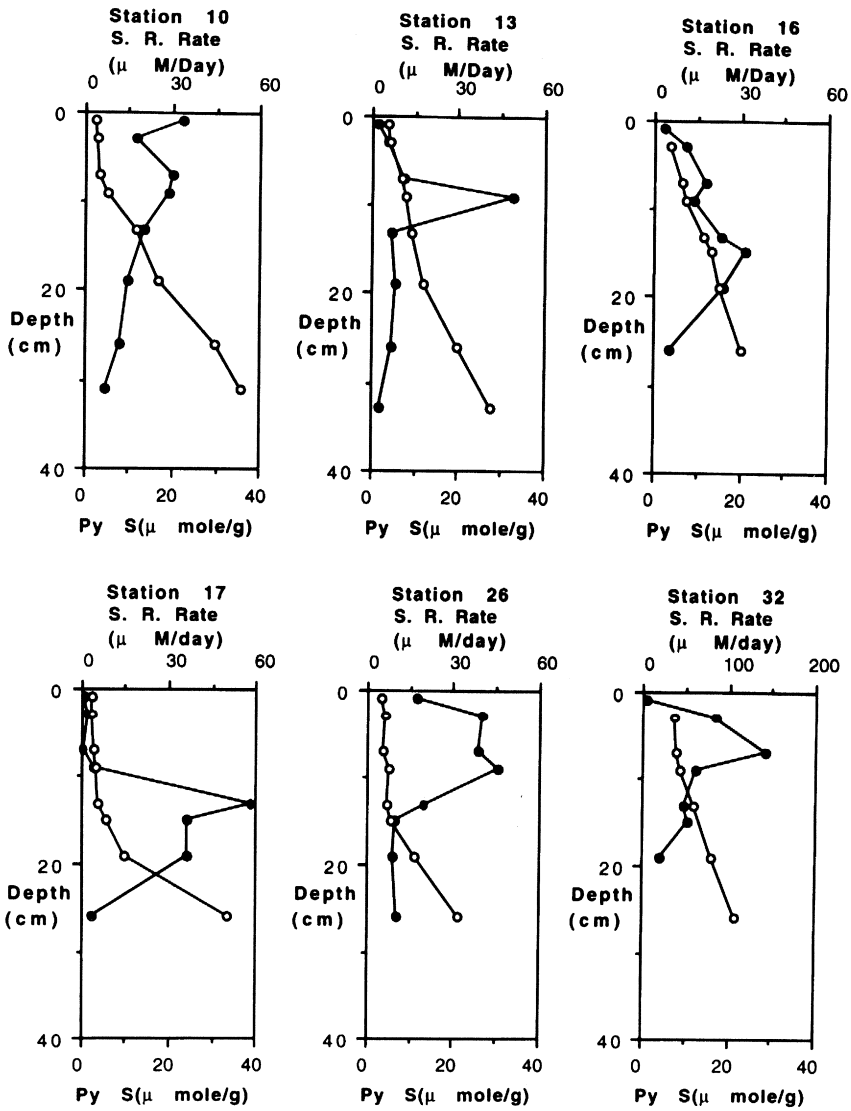

Fig. 2. Sulfate reduction rate (●) and pyrite-sulfur content (○) versus depth in the study area.

due to rapid reaction between dissolved sulfide and iron oxide/oxyhydroxide minerals (Canfield *et al.*, 1992).

Organic carbon and Pore water sulfate

A slight sulfate depletion was observed in the upper 30 cm (Fig. 3). Station 29 showed the most dramatic sulfate depletion, down to a low value of 5 mM (Appendix). The sulfate profiles resembled those observed in the Amazon inner shelf mud (Aller *et al.*, 1986). The sluggish sulfate depletion was probably a result of bioturbation and/or physical mixing since the top 12 cm sediment showed no change in ^{210}Pb activity in most stations.

Organic carbon concentration varied from 0.3% to 0.6% by weight, higher than the average outer shelf sediments organic carbon concentration of ~0.2% (Lin *et al.*, 1992). Generally, organic carbon decreased with increasing depth (station 26,

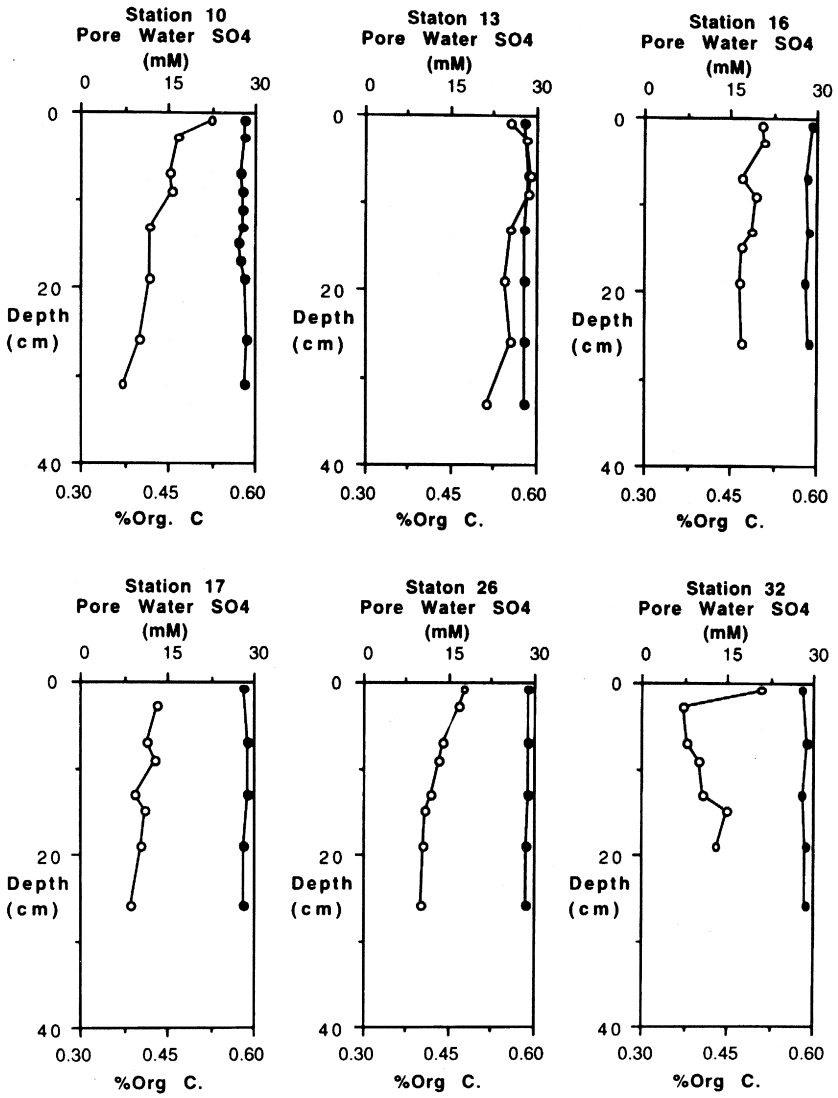

Fig. 3. Organic carbon (○) and pore water dissolved sulfate (●) versus depth in the study area.

Fig. 3). Irregular variation was observed in station 32 where organic carbon decreased rapidly within the top 5 cm and later increased with depth.

Oxalate iron and Reactive iron

The concentrations of oxalate extractable iron and cold acid extractable iron (reactive iron) range from 80–120 μmol/g and 200–260 μmol/g, respectively (Fig. 4). There are no regular changes with depth for the cold acid iron. The concentrations of reactive iron were much higher than the FOAM sediments (Canfield *et al.*, 1992) and approximately 30-50% higher than the Gulf of Mexico sediments (Lin, 1989). An oxalate iron maximum was often observed on top of the pyrite-sulfur (station 26, Figs. 2 and 4). The concentrations of oxalate iron, in general, were higher than the Long Island Sound sediments but lower than the Mississippi River Delta sediments (Canfield, 1989b).

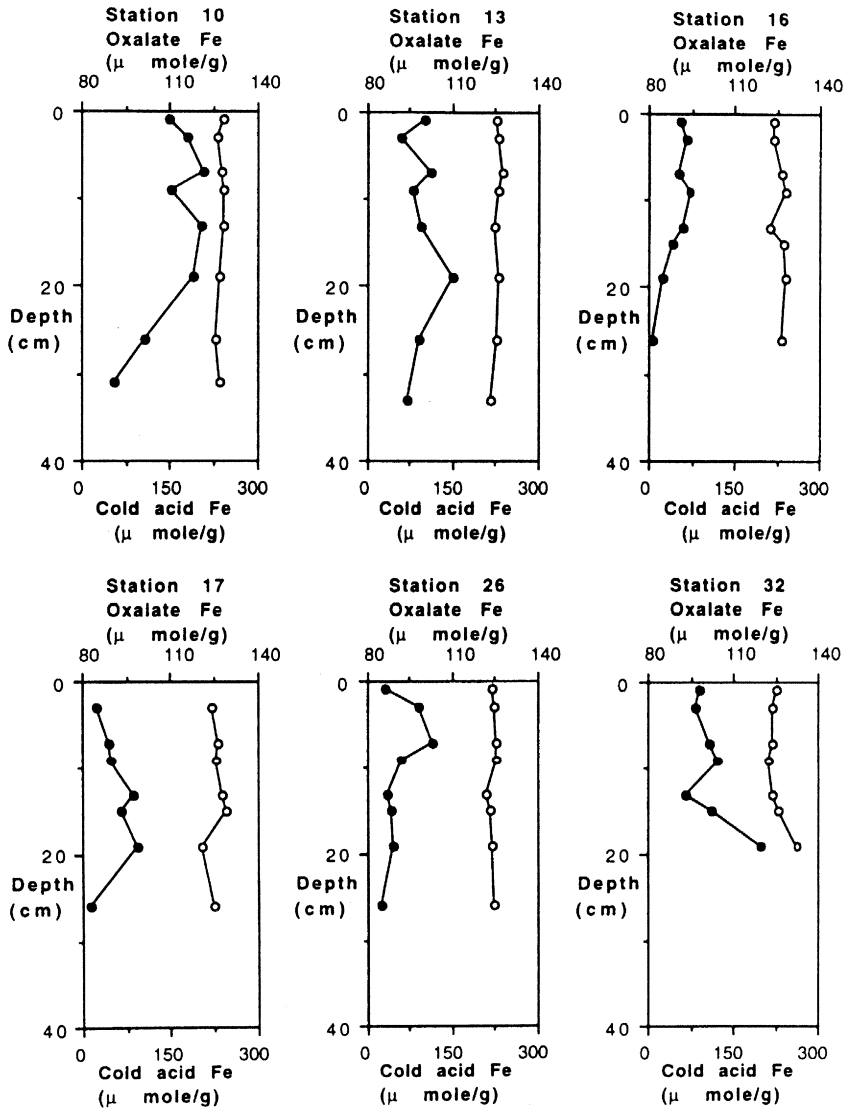

Fig. 4. Cold acid extractable iron (○) and oxalate iron (●) versus depth in the study area.

Discussion

The supply of organic material to the sediment is often considered to be the primary controlling mechanism for diagenetic iron sulfide mineral formation in normal marine sediments. Iron and sulfate limitation usually become important only in euxinic and non-marine sedimentary environments (Berner, 1970). The importance of iron in pyrite formation was recently raised by Canfield and Raiswell (1991) who indicated that iron limitation should occur in most continental margin sediments where sulfate reduction rates often far exceed the burial rate of iron. This study indicates that organic carbon, instead of iron, is the factor in controlling pyrite formation in the East China Sea continental shelf sediments. Abundant iron oxides and sulfate were observed in sediments and pore waters of the study region, which suggests that these two parameters were unlikely to play an important role in determining pyrite formation.

Sulfate reduction rates plotted against

sedimentation rate fall underneath the "iron band" of Canfield and Raiswell (1991). The reason for this deviation is the unusual accumulation of abundant reactive iron in the East China Sea continental shelf sediments. As a result, more reactive iron is available than the sulfide production in this region.

Organic Carbon as Limiting Factor

Organic carbon is the primary factor in controlling sulfate reduction in the study region. Both the direct incubation rate measurements and the C/S ratio indicate that organic carbon is limiting pyrite formation in the East China Sea continental shelf sediments. Integrated sulfate reduction rate increases as the organic carbon concentration increases in sediments (r^2 = 0.73, Fig. 5). Sulfate reduction rate increased threefold with an increase of organic carbon from 0.37% to 0.60%. As more organic carbon becomes available, sulfate reduction rate increases accordingly. A similar correlation was also observed in the Mississippi River Delta sediments (Lin and Morse, 1991) where higher sediment deposition rates enhance the availability of fresh organic matter for the sulfate reducing bacteria. The organic carbon, therefore, ultimately limits the rate of sulfate reduction.

In addition, the C/S ratio (Fig. 6) also demonstrates that organic carbon limits the amounts of pyrite formed in the sediments. In the study region, C/S decreased rapidly from about ~20–60 to a typical normal marine ratio at a depth of approximately 20 cm. The decrease of C/S ratio is a result of the pyrite formation at depth from the deposition of the reactive organic matter. This C/S ratio of ~2.8 was observed in a number of modern marine sediments (Leventhal, 1983; Berner, 1970, 1982; Goldhaber and Kaplan, 1974). According to Berner (1984), a constant fraction of the initially deposited organic matter is utilized by sulfate reduction which in turn determines the amount of pyrite formation and burial of non-utilized carbon. As a result, a constant C/S ratio of ~2.8 indicates that the labile organic matter limits the amount of pyrite formed in normal oxygenated marine environment. Therefore, the C/S ratio of approximately 3 at depth in the study region clearly indicates an organic carbon limitation.

Iron as Limiting Factor

Considering the low organic carbon deposition in the marine sediments, organic carbon is nor-

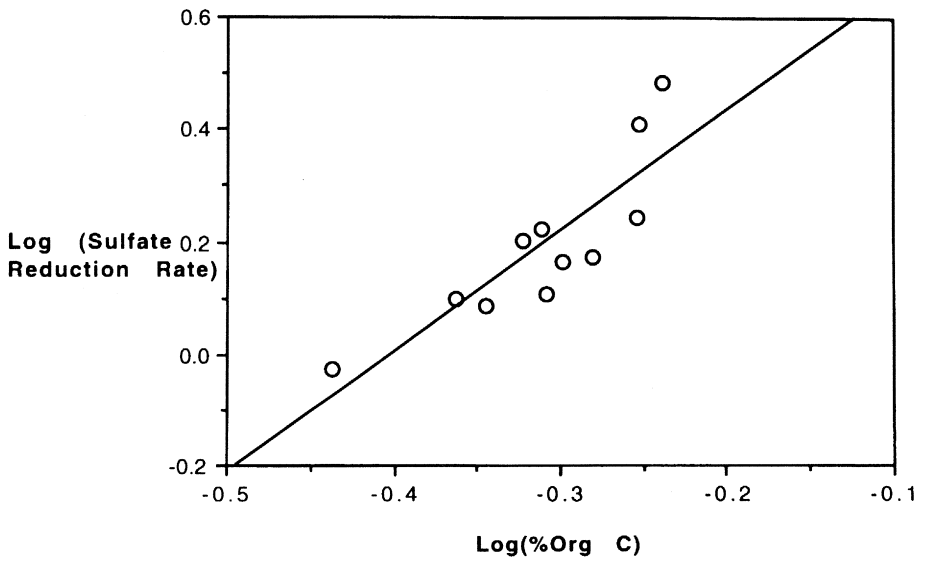

Fig. 5. Integrated sulfate reduction rate (m mole/m^2/day) increases with increasing organic carbon concentration. Correlation coefficient (r^2) is 0.732.

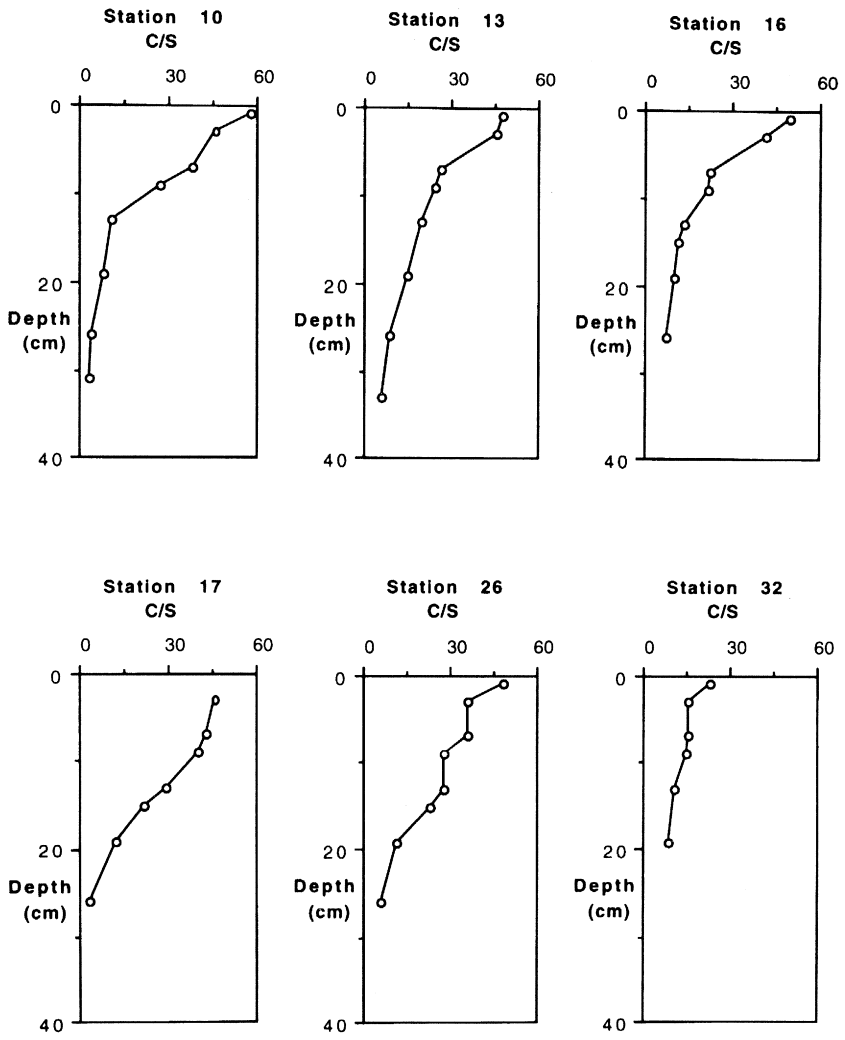

Fig. 6. C/S (organic carbon/pyrite sulfur) ratio versus depth in the study area. C/S ratios of approximately 3 were observed at depth.

mally the primary factor in dominating the rate of sulfate reduction in anoxic sediments. Recent studies, however, indicated that iron may also play an important role in determining the extent of pyrite formation in normal shelf sediments (Canfield *et al.*, 1992; Canfield and Raiswell, 1991; Aller *et al.*, 1986). Canfield and Raiswell (1991) proposed that iron, instead of organic carbon, limits iron sulfide mineral formation in the continental margin sediment since the production of sulfide often exceeds the accumulation of reactive iron. Canfield *et al.* (1992) further showed that the reactivity between iron minerals and sulfide varies to a large extent. The reaction half life for the least crystalline iron mineral, ferrihydrite, is only about ~4 hours. The sheet silicate minerals are longer with a half life of 10^5 years whereas augite and amphibole will take at least 10^6 years to react with dissolved sulfide. On the grounds that most readily reactive iron oxides are usually exhausted when sediment reach the base of the sulfate reduction zone, they argued that iron will limit pyrite formation in continental margin sediments where sulfide production exceeds reactive iron

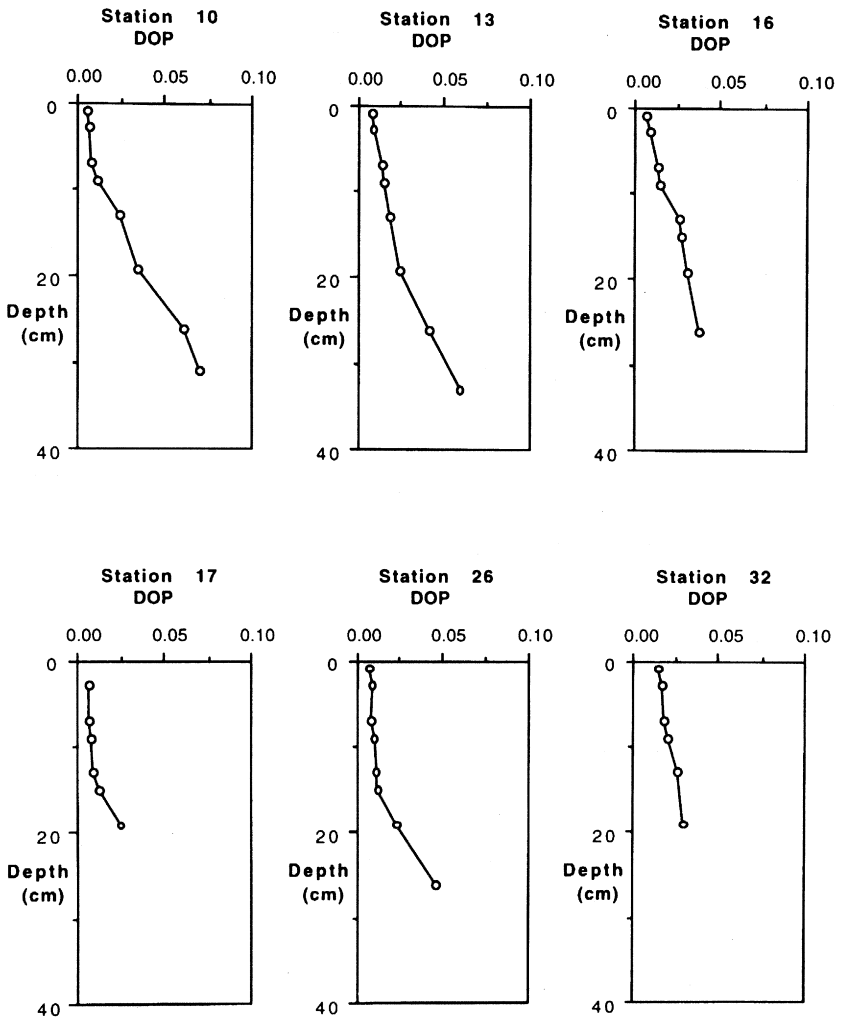

Fig. 7. Degree of pyritization versus depth in the study area. DOP was relatively low in the sediment.

deposition rate (Canfield and Raiswell, 1991).

Although iron is limited as reported in some of the continental margin sediments (e.g. the FOAM site in Canfield (1988), Kau Bay, Indonesia in Middleburg (1991), and Baltic Sea in Boesen and Postma (1988)), it is not a limiting factor of pyrite formation in the East China Sea continental shelf sediments. This is because reactive iron is very high in the study region (Fig. 4), approximately 30–50% higher than that in the Gulf of Mexico continental margin sediments (Lin, 1989), a positive indication that reactive iron is not in short supply and does not limit pyrite formation. In addition, the DOP values never exceeded ~16% calculated from either cold acid extractable iron (Fig. 7) or oxalate extractable iron based on Canfield *et al.* (1992). This low DOP indicates that iron is available for the pyrite formation.

Canfield *et al.* (1992) indicated that iron limitation does not occur in sediments where ferrihydrite and lepidocrocite minerals are present, even in environments with fresh organic matter. The oxalate extractable iron concentrations (ferrihydrite and lepidocrocite, Canfield, 1989b) were very high, ranging between 80 and 120 μmol/g in the East China Sea shelf sediments

(Fig. 4). The sedimentation rates were between 0.2–0.7 cm/year in this region. When sulfate reduction rates are plotted versus sedimentation rates, all the East China Sea shelf sediments fall underneath the "iron band" of Canfield and Raiswell (1991). Thus, although the reactivity of iron oxide minerals may be an important factor in controlling pyrite formation in some environments (Canfield *et al.*, 1992), the abundance of ferrihydrite and lepidocrocite in the East China Sea continental shelf sediments evidently demonstrate that iron is not the major factor limiting pyrite formation in the study region.

Conclusions

Sulfate reduction and iron sulfide mineral formation are common processes in the East China Sea continental shelf sediments. Pyrite formation was found to be limited by the available organic carbon. Iron limitation was not observed in the East China Sea continental shelf due to the high concentrations of the least crystalline iron oxide minerals.

Sulfate reduction rate increased with increasing organic carbon concentration. C/S ratio in the region was similar to the average normal marine sediments. Both demonstrate that organic carbon controls the iron sulfide mineral formation in the study region. The low DOP values and abundant highly reactive ferrihydrite and lepidocrocite iron minerals indicate that iron was not limited in the East China Sea continental shelf.

Acknowledgments—The authors thank Dr. Rob Raiswell and an anonymous reviewer for their constructive comments. We also thank the captain and crew of "Ocean Researcher-I" for their assistance during our sample collection. This research was funded by the National Science Council, R.O.C. (NSC-842611M002A008K2 and 830209M002A013K to SL).

References

Aller, R. C., Mackin, J. E. and Cox, R. T., Jr. (1986) Diagenesis of Fe and S in Amazon inner shelf muds: apparent dominance of Fe reduction and implications for the genesis of ironstones. *Cont. Shelf Res.* **6**, 263–289.

Berner, R. A. (1970) Sedimentary pyrite formation. *Amer. J. Sci.* **268**, 1–23.

Berner, R. A. (1982) Burial of organic carbon and pyrite sulfur in the modern ocean: its geochemical and environmental significance. *Amer. J. Sci.* **282**, 451–473.

Berner, R. A. (1984) Sedimentary pyrite formation: an update. *Geochim. Cosmochim. Acta* **48**, 605–615.

Berner, R. A. (1989) A biogeochemical cycles of carbon and sulfur and their effect on atmospheric oxygen over Phanerozoic time. *Paleogeog. Paleoclimat. Paleoecol.* **75**, 97–122.

Berner, R. A. (1991) A model for atmospheric CO_2 over Phanerozoic time. *Amer. J. Sci.* **291**, 339–376.

Berner, R. A. and Raiswell, R. (1983) Burial of organic carbon and pyrite sulfur in sediments over Phanerozoic time: a new theory. *Geochim. Cosmochim. Acta* **47**, 855–862.

Berner, R. A. and Raiswell, R. (1984) C/S method for distinguishing freshwater from marine sedimentary rocks. *Geology* **12**, 365–368.

Boesen, C. and Postma, D. (1988) Pyrite formation in anoxic environments of the Baltic. *Amer. J. Sci.*, **288**, 575–603.

Canfield, D. E. (1988) Sulfate reduction and the diagenesis of iron in anoxic marine sediment. Ph.D. Dissertation, Yale University.

Canfield, D. E. (1989a) Sulfate reduction and oxic respiration in marine sediments: implications for organic carbon preservation in euxinic environments. *Deep Sea Res.* **36**, 121–138.

Canfield, D. E. (1989b) Reactive iron in marine sediments. *Geochim. Cosmochim. Acta* **53**, 619–632.

Canfield, D. E. and Raiswell, R. (1991) Pyrite formation and fossil preservation. *Taphonomy: Releasing the Data Locked in the Fossil Record, Topics in Geobiology, Vol. 9* (Allison, P. A. and Briggs, D. E., eds.), 337–387, Plenum Press, New York.

Canfield, D. E., Raiswell, R. and Bottrell, S. (1992) The reactivity of sedimentary iron minerals toward sulfide. *Amer. J. Sci.* **292**, 659–683.

Canfield, D. E., Raiswell, R., Westrich, J. T., Reaves, C. M. and Berner, R. A. (1986) The use of chromium reduction in the analysis of reduced inorganic sulfur in sediments and shales. *Chem. Geol.* **54**, 149–155.

Cao, P., Huo, F., Gu, G. and Zhou, Y. (1989) Relationship between suspended sediments from the Changjiang estuary and the evolution of the embayed muddy coast of Zhejinag Province. *Acta Oceanol. Sinica* **8**, 273–283.

Cornwell, J. C. and Morse, J. W. (1987) The Characterization of iron sulfide minerals in marine

sediments. *Mar. Chem.* **22**, 193–206.

Dean, W. E. and Arthur, M. A. (1989) Iron-sulfur-carbon relationships in organic-carbon-rich sequences I: Cretaceous Western Interior Seaway. *Amer. J. Sci.* **289**, 708–743.

Gautier, D. L. (1986) Isotopic composition of pyrite: Relationship to organic matter type and iron availability in some North American Cretaceous shales. *Chem. Geol.* **65**, 293–303.

Goldhaber, M. B. and I. R. Kaplan (1974) The sulfur cycle. *The Sea, Vol. 5* (Goldberg, E. D., ed.), 569–655, Wiley.

Jorgensen, B. B. (1978) A comparison of methods for the quantification of bacterial sulfate reduction in coastal marine sediments. III. Estimation from chemical and bacteriological field data. *Geomicrobiol. J.* **1**, 49–64.

Jorgensen, B. B. (1982) Mineralization of organic matter in the sea bed—the role of sulfate reduction. *Nature* **296**, 643–645.

Kokot, S., King, G., Leller, H. R. and Massart, D. L. (1992) Application of chemometrics for the selection of microwave digestion procedures. *Anal. Chim. Acta* **268**, 81–94.

Lee, H. J. and Chough, S. K. (1989) Sediment dispersion, dispersal and budget in the Yellow Sea. *Mar. Geol.* **87**, 195–205.

Leventhal, J. S. (1983) An interpretation of carbon and sulfur relationships in Black Sea sediments as indicators of environment of deposition. *Geochim. Cosmochim. Acta* **47**, 133–137.

Li, C., Chen, G., Yao, M. and Wang, P. (1991) The influences of suspended load on the sedimentation in the coastal zones and continental shelves of China. *Mar. Geol.* **96**, 341–352.

Lin, S. (1989) Environmental controls on sulfate reduction and iron sulfide mineral formation. Ph.D. Dissertation, Texas A&M University, 189 pp.

Lin, S., Liu, K. K., Chen, M. P., Chen, P. and Chang, F. Y. (1992) Distribution of organic carbon in the KEEP area continental margin sediments. *TAO* **3**, 365–378.

Lin, S. and Morse, J. W. (1991) Sulfate reduction and iron sulfide mineral formation in Gulf of Mexico anoxic sediments. *Amer. J. Sci.* **291**, 55–89.

Middleburg, J. J. (1991) Organic carbon, sulfur, and iron in recent semi-euxinic sediments of Kau Bay, Indonesia. *Geochim. Cosmochim. Acta* **55**, 815–828.

O'Dell, J. W., Pfaff, J. D., Gales, M. E. and McKee, G. D. (1984) The determination of inorganic anions in water by ion chromatography-method 300.0. U.S. EPA 600/4.84.017, 5 pp.

Raiswell, R. and Berner, R. A. (1985) Pyrite formation in euxinic and semi-euxinic sediments. *Amer. J. Sci.* **285**, 710–724.

Reeburgh, W. S. (1983) Rates of biogeochemical processes in anoxic sediments. *Ann. Rev. Earth Planet. Sci.* **11**, 269–298.

Sternberg, R. W., Larsen, L. H. and Miao, Y. (1985) Tidally driven sediment transport on the East China Sea continental shelf. *Cont. Shelf Res.* **5**, 105–120.

Appendix Table. Analytical data

Station ID	Depth (cm)	SO_4 (mM)	Py-S (μmol/g)	Org. C (wt%)	$CaCO_3$ (wt%)	React. Fe (μmol/g)	Total Fe (μmol/g)	Sulf. Red. Rate (μM/day)
9	1	29.0	2.90	0.349	11.3	250	—	—
	3	29.1	—	0.418	9.47	251	—	—
	7	29.1	3.00	0.425	10.1	244	—	—
	9	28.7	6.60	0.387	9.62	243		—
	13	28.8	11.1	0.362	9.30	238	—	—
	19	28.0	14.1		10.3	241	—	—
	26	27.9	16.4	0.347	9.72	234	—	—
	33	27.0	20.4	0.373	9.18	241	—	—

Appendix Table. (continued)

Station ID	Depth (cm)	SO_4 (mM)	Py-S (μmol/g)	Org. C (wt%)	$CaCO_3$ (wt%)	React. Fe (μmol/g)	Total Fe (μmol/g)	Sulf. Red. Rate (μM/day)
10	1	28.3	2.83	0.525	9.04	241	697	10.4
	3	28.2	3.18	0.467	8.09	232	678	4.54
	7	27.7	3.74	0.453	8.47	237	676	8.69
	9	27.9	5.32	0.456	8.50	242	691	8.00
	13	28.0	11.9	0.421	9.63	243	708	5.55
	19	28.2	16.8	0.418	10.0	236	697	3.32
	26	28.5	29.5	0.401	10.7	228	659	2.16
	31	28.3	35.5	0.370	10.3	235	670	0.892
11	1	28.4	3.85	0.491	7.89	215	707	5.58
	3	28.4	3.76	0.539	7.35	232	683	10.3
	7	28.2	3.73	0.498	7.26	232	690	9.07
	9	26.9	—	0.507	7.40	245	710	7.90
	13	27.2	8.52	0.463	8.85	240	681	9.78
	15	27.2	9.12	—	—	—	703	—
	19	27.6	12.2	0.443	8.59	237	690	5.14
	26	27.7	20.2	0.451	7.87	241	661	0.556
	33	28.5	26.4	—	—	—	642	0.387
12	1	27.7	3.56	0.581	6.35	221	—	—
	3	27.9	3.76	0.537	6.38	228	—	—
	7	28.1	5.67	0.512	6.23	237	—	—
	9	28.0	7.60	0.515	6.26	236	—	—
	13	28.2	10.0	0.492	6.56	229	—	—
	15	27.8	10.3	0.483	6.46	224	—	—
	19	27.0	14.6	0.497	6.62	236	—	—
	26	27.1	18.9	0.461	7.34	229	—	—
13	1	28.1	3.64	0.557	5.87	227		1.06
	3	28.2	3.98	0.584	5.58	233	726	2.73
	7	28.5	7.03	0.591	5.95	237	738	4.77
	9	28.1	7.54	0.586	6.23	231	709	21.7
	13	28.0	8.91	0.556	6.01	225	729	2.64
	19	27.8	11.7	0.546	5.81	232	761	3.23
	26	27.8	19.9	0.555	5.97	230	738	2.60
	33	27.9	27.6	0.514	6.05	217	737	0.902
14	1	28.4	6.14	0.635	5.83	223	—	—
	3	28.1	—	0.552	5.90	221	—	—
	7	27.8	6.97	0.570	6.10	223	—	—
	9	28.0	—	0.571	6.64	227	—	—
	13	27.6	11.9	0.570	6.61	204	—	—
	15	27.9	—	0.549	7.19	195	—	—
	19	27.9	31.5	0.533	6.96	199	—	—
	26	28.0	27.6	0.557	6.50	197	—	—
	33	28.2	28.2	0.505	5.93	196	—	—
	40	27.7	41.6	0.516	6.84	—	—	—
15	1	27.2	4.04	0.559	5.82	220	712	10.1
	3	27.7	—	0.522	6.54	229	740	6.74
	7	25.9	6.72	0.568	6.18	230	752	12.6
	9	24.5	9.76	0.574	6.57	236	731	5.90
	13	29.3	12.3	0.523	6.79	232	739	9.39
	15	27.5	15.3	0.612	7.38	238	600	8.15
	19	27.7	13.7	0.537	6.71	236	737	9.30
	26	27.4	19.1	0.542	6.16	228	730	5.59

Appendix Table. (continued)

Station ID	Depth (cm)	SO_4 (mM)	Py-S (μmol/g)	Org. C (wt%)	$CaCO_3$ (wt%)	React. Fe (μmol/g)	Total Fe (μmol/g)	Sulf. Red. Rate (μM/day)
16	1	29.2	3.16	0.503	6.81	218	661	1.30
	3	28.9	3.86	0.509	6.90	217	664	4.48
	7	28.4	6.56	0.471	6.47	232	685	6.33
	9	28.4	7.13	0.494	6.22	239	671	4.79
	13	28.5	11.4	0.489	6.25	212	706	7.99
	15	28.1	13.0	0.472	6.32	235	699	10.7
	19	27.9	14.8	0.468	6.07	237	688	8.43
	26	28.5	17.8	0.470	6.17	232	695	1.75
17	1	28.2	2.54	—	—	—	717	0.333
	3	28.5	2.95	0.433	7.78	222	634	0.853
	7	28.9	3.04	0.415	7.85	230	611	0.182
	9	28.8	3.41	0.431	7.26	228	636	1.50
	13	29.0	4.24	0.397	5.83	240	644	18.0
	15	28.8	6.02	0.411	7.39	247	621	11.2
	19	28.4	10.2	0.406	8.63	204	634	11.1
	26	28.4	33.1	0.390	11.8	—	609	1.10
	33	—	—	—	—	223	—	—
18	1	27.6	3.76	0.499	8.67	239	—	—
	3	28.5	4.18	0.428	8.50	247	—	—
	7	27.8	5.03	0.419	8.90	257	—	—
	9	27.7	8.24	0.411	8.54	258	—	—
	13	28.3	9.70	0.409	11.2	254	—	—
	15	26.2	—	0.375	11.2	—	—	—
	19	29.0	11.3	0.359	11.4	232	—	—
	26	28.0	30.3	0.356		249	—	—
19	1	28.9	3.31	0.365	10.5	247	837	14.3
	3	28.8	4.41	0.386	10.7	258	574	10.5
	5	—	3.66	—	—	—	582	—
	7	28.	4.25	0.362	10.0	248	578	6.87
	9	28.7	5.06	0.373	10.4	237	572	4.88
	13	29.1	6.99	0.358	12.6	237	593	3.72
	15	28.4	8.27	0.353	10.1	255	592	2.69
	26	—		—	—	224	—	—
21	1	28.8	2.92	0.364	10.0	221	—	—
	3	28.4	3.43	0.341	9.39	233	—	—
	7	28.9	—	0.356	9.21	238	—	—
	9	28.1	4.72	0.400	8.73	243	—	—
	13	28.5	6.11	0.336	12.1	238	—	—
	19	28.0	12.3	0.319		247	—	—
	26	28.3	31.7	0.357	9.90	249	—	—
	33	27.9	27.8	0.307	10.5	246	—	—
23	1	27.8	2.54	0.489	7.17	221	630	2.75
	3	27.8	3.03	0.466	7.53	228	583	—
	7	27.9	2.95	0.455	7.33	230	649	8.42
	9	28.8	4.07	0.468	6.96	230	646	6.40
	13	28.1	3.04	0.468	7.34	230	668	9.46
	19	28.1	3.63	0.416	7.79	228	644	7.33
	26	28.4	10.9	0.396	8.95	243	628	2.70
	33	27.9	27.7	—	—	238	651	2.69

Appendix Table. (continued)

Station ID	Depth (cm)	SO_4 (mM)	Py-S (μmol/g)	Org. C (wt%)	$CaCO_3$ (wt%)	React. Fe (μmol/g)	Total Fe (μmol/g)	Sulf. Red. Rate (μM/day)
24	1	28.4	3.25	0.631	10.0	232	—	—
	3	28.9	—	0.501	6.08	213	—	—
	7	28.8	3.42	0.502	6.11	235	—	—
	9	28.7	3.11	0.504	6.03	229	—	—
	13	27.7	4.25	0.525	6.45	218	—	—
	19	28.6	9.88	0.510	6.12	230	—	—
	26	28.3	16.1	0.516	5.75	224	—	—
	31	27.7	20.0	0.521	5.61	222	—	—
25	1	28.4	2.77	0.578	6.38	220	619	2.46
	3	28.9	3.71	0.266	8.73	223	647	43.6
	7	29.0	3.73	0.559	6.14	232	653	12.2
	9	28.2	3.40	0.546	6.64	230	660	10.2
	13	28.0	3.63	0.519	6.39	237	663	11.1
	15	28.5	3.45	0.449		230	652	9.29
	19	28.2	6.07	0.242	9.73	233	798	5.72
	26	28.7	8.10	0.503	7.51	224	634	6.78
26	1	29.0	3.06	0.476	7.97	221	596	5.45
	3	29.0	4.06	0.466	7.46	225	605	14.4
	7	28.9	3.81	0.439	7.40	228	638	12.2
	9	28.7	4.95	0.434	7.48	230	643	14.2
	13	28.9	4.68	0.418	7.58	213	601	5.97
	15		5.65	0.408	7.76	219	612	2.27
	19	28.5	10.9	0.407	7.78	223	632	2.12
	26	29.8	21.4	0.403	7.42	224	621	1.88
27	1	29.4	3.04	0.452	8.28	224	581	4.32
	3	28.8	—	0.418	8.23	231	577	11.1
	7	28.6	3.61	0.402	8.04	229	594	8.01
	9	29.0	3.70	0.411	8.40	224	597	6.01
	13	29.1	6.95	0.411	7.79	220	592	3.46
	15	28.6	—	0.378	8.21	227	590	3.61
	19	28.4	7.54	0.184	10.0	228	571	3.07
	26	28.5	7.54	0.362	8.46	231	585	1.16
	33	—	16.9	—	—	—	580	—
29	11	29.8	66.5	0.46	8.83	180	—	—
	14	29.4	—	0.47	10.2	210	—	—
	17	28.9	66.2	—	—	—	—	—
	20	29.2	—	0.43	10.4	186	—	—
	23	28.9	—	—	—	235	—	—
	29	29.0	67.9	0.50	10.3	—	—	—
	42	27.2	—	0.45	8.80	—	—	—
	51	28.4	97	0.54	9.33	—	—	—
	101	25.9	69.0	0.16	8.13	147	—	—
	151	17.5	—	—	—	—	—	—
	201	12.5	51.6	0.13	6.01	131	—	—
	251	10.0	—	—	—	—	—	—
	301	6.02	85.0	0.10	6.5	114	—	—
	351	5.55	110	—	—	195	—	—

Appendix Table. (continued)

Station ID	Depth (cm)	SO_4 (mM)	Py-S (μmol/g)	Org. C (wt%)	$CaCO_3$ (wt%)	React. Fe (μmol/g)	Total Fe (μmol/g)	Sulf. Red. Rate (μM/day)
32	1	27.9	6.86	0.508	9.14	227	536	1.50
	3	28.3	7.37	0.372	9.67	218	519	26.8
	7	29.1	7.74	0.378	9.83	217	523	41.6
	9	28.5	8.56	0.398	9.37	212	542	16.8
	13	28.1	11.7	0.405	9.68	218	552	13.2
	15	28.6	—	0.451	9.06	228	586	15.5
	19	28.5	15.9	0.430	8.62	231	575	5.93
	26	28.5	21.4	—	—	—	573	—